

# VU Research Portal

## Visualizing the Shrinking Brain: Longitudinal MR Studies in the Spectrum of Cognitive Decline

Sluimer, J.D.

2011

### **document version**

Publisher's PDF, also known as Version of record

[Link to publication in VU Research Portal](#)

### **citation for published version (APA)**

Sluimer, J. D. (2011). *Visualizing the Shrinking Brain: Longitudinal MR Studies in the Spectrum of Cognitive Decline*. [PhD-Thesis - Research and graduation internal, Vrije Universiteit Amsterdam].

### **General rights**

Copyright and moral rights for the publications made accessible in the public portal are retained by the authors and/or other copyright owners and it is a condition of accessing publications that users recognise and abide by the legal requirements associated with these rights.

- Users may download and print one copy of any publication from the public portal for the purpose of private study or research.
- You may not further distribute the material or use it for any profit-making activity or commercial gain
- You may freely distribute the URL identifying the publication in the public portal

### **Take down policy**

If you believe that this document breaches copyright please contact us providing details, and we will remove access to the work immediately and investigate your claim.

### **E-mail address:**

[vuresearchportal.ub@vu.nl](mailto:vuresearchportal.ub@vu.nl)

# Chapter 2

## **Amnestic mild cognitive impairment: Structural MRI findings predictive of conversion to Alzheimer's disease**

American Journal of Neuroradiology 2008

G.B. Karas  
J.D. Sluimer  
R. Goekoop  
W.M. van der Flier  
S.A.R.B. Rombouts  
Ph. Scheltens  
F. Barkhof

### Abstract

**Background and Purpose:** Mild cognitive impairment (MCI) is by many considered a prodromal phase of Alzheimer's disease (AD). We used voxel-based morphometry (VBM) to find out whether structural differences on MRI could offer insight about the development of clinical AD in patients with amnesic MCI at three years follow-up.

**Methods:** Twenty-four amnesic MCI patients were included. After three years 46% had progressed to AD (n=11, age [72.7, SD 4.8]; sex [women/men] 8/3). For 13 patients (age [72.4, SD 8.6]; sex [women/men] 10/3) the diagnosis remained MCI. Baseline MRI at 1.5T included a coronal heavily T1-weighted 3D gradient echo sequence. Localized grey matter differences were assessed with VBM.

**Results:** The converters had less grey matter volume in medial (including the hippocampus) and lateral temporal lobe structures, parietal lobe structures and lateral temporal lobe structures. After correction for age, gender, total grey matter volume and neuropsychological evaluation, left-sided atrophy remained statistically significant. Specifically, converters had more left parietal atrophy (angular gyrus and inferior parietal lobule) and left lateral temporal lobe atrophy (superior and middle temporal gyrus) than stable MCI patients.

**Conclusion:** By studying two MCI populations, converters versus non-converters, we found atrophy beyond the medial temporal lobe to be characteristic of MCI patients who will progress to dementia. Atrophy of structures such as the left lateral temporal lobe and left parietal cortex may independently predict conversion.

## Introduction

The term mild cognitive impairment was coined to describe individuals not yet fulfilling the criteria of Alzheimer's disease, but who evidently do not have a normal cognitive profile compared to their contemporaries.<sup>1</sup> The annual conversion rate of MCI patients is generally believed to lie around 10-15%, meaning that by three years half of the patients with MCI will probably have developed clinical AD.<sup>2</sup> If drugs become available that could influence the course of the disease, it is evident that these should be administered at the earliest stage at which a diagnosis can be made with certainty. Hence, clinical, biological and imaging markers are needed to detect that earliest stage of underlying pathology.

Previous MRI studies assessing the predictive value of structural brain changes for AD focused on medial temporal lobe atrophy (MTA).<sup>3,4</sup> Brains of patients with Alzheimer's disease exhibit more atrophy in the medial temporal lobe, thalamus, superior temporal gyrus, parietal association cortex and cingulate gyrus, than patients with MCI.<sup>5-8</sup> Some of these brain atrophy locations might provide additional independent information about risk of conversion<sup>9</sup>; conversion from MCI to AD has already been associated with hippocampal and entorhinal volume loss<sup>10</sup> and with hippocampal shape changes.<sup>11</sup> We adopted a longitudinal approach, in which we followed up a study group for three years and then compared the baseline MRI scans. Voxel-based morphometry was chosen as the post-processing method in order to avoid a priori hypotheses.

## **Patients and Methods**

### **Patient inclusion**

Twenty-five amnesic MCI patients were prospectively selected from the Alzheimer Center at the VU Medical Center, Amsterdam, The Netherlands. Due to image pipeline failure one patient had to be excluded, leaving 24 patients for analysis. MCI patients were diagnosed according to the Petersen criteria with a slowly progressive memory decline without the involvement of another domain of cognitive function, that did not interfere significantly with activities of daily living.<sup>2</sup> Inclusion of an individual in the study required mini-mental state examination (MMSE) score of 24 and higher.<sup>12</sup> Follow-up ending for this study was set at three years after inclusion and diagnosis of AD was made according to the NINCDS-ARDRA criteria.<sup>13</sup> All patients received a diagnostic battery comprising of mini-mental state examination - MMSE<sup>12</sup>, clinical dementia rating - CDR<sup>14</sup> and NYU-paragraph recall tests, which were used for cognitive profiling. The study had approval of the review board of the committee of medical ethics of the VU University Medical Center in Amsterdam, The Netherlands. All patients provided informed consent according to the Declaration of Helsinki under supervision of a lawful caretaker during a screening visit in which the procedure was explained and contraindications were checked.

### **MRI Data Acquisition**

Imaging was carried out on a 1.5 T Sonata scanner (Siemens AG, Erlangen, Germany), using a standard circularly polarized head coil with foam padding to restrict head motion. A heavily T1-weighted structural 3D sequence was employed to obtain high resolution images (MP-RAGE; inversion time: 300s, TR = 15 ms; TE = 7 ms; flip angle = 8°; 160 coronal slices, 1x1x1.5 mm voxel dimensions). Additional to the structural MRI protocol the patients also received FLAIR and gradient-echo weighted sequences to exclude significant vascular pathology or microbleeds which might interfere with either the diagnosis of pure amnesic MCI or cause the segmentation of the T1-weighted images to be sub-optimal.

### **Visual Scoring**

In order to have an absolute and not a relative measure of hippocampal atrophy the MTA was visually scored on the coronal images using a well validated scale, medial temporal atrophy scale.<sup>15,16</sup> According to the scale, MTA scores evaluate the medial temporal lobe structures, encompassing the hippocampus proper, dentate gyrus, subiculum, parahippocampal gyrus and the volume of the surrounding cerebrospinal fluid (CSF) spaces, especially the temporal horn of the lateral ventricle and the choroid fissure. MTA scores range from 0 (no atrophy) to 4 (severe atrophy) on each side. Visual scores from left and right were averaged. The rater (J.S.) was blinded to diagnosis or other clinical variables of the patients, and trained using our standard training set (19 brains, none belonging to the study's dataset) to meet consistency requirements according to our standard operating procedure. The intrarater weighted Cohen's kappa was 0.93 and interrater weighted Cohen's kappa was 0.91 (against internally established gold-standard).

### **SIENAX**

Global grey matter volume was estimated with a cross-sectional atrophy estimation method called SIENAX.<sup>17</sup> Briefly, scans were affinely (12 parameters) registered to standard Montreal Neurological Institute space (average template of 152 healthy adult brains), the skull was extracted and grey matter was segmented based on signal intensity and a voxel-connectivity algorithm. Subsequently, global grey matter volumes were corrected for scaling and scanner errors by using the extracted skull as a constant variable and partial volume effects were incorporated into the model. The resulting grey matter volumes were then expressed as cubic centimeters (cm<sup>3</sup>).

## **Voxel-based Morphometry**

### **Preprocessing**

Localized grey matter differences were assessed with VBM<sup>18</sup>, implemented as described previously.<sup>8,19</sup> A detailed algorithm with the image processing settings of the proposed VBM scheme is shown in table 1. MRI scans were brought into standard reference anatomical space using an affine 12-parameter registration and with the MNI template as target. We chose not to perform nonlinear registration since Jacobian analysis of SPM-basis function warped images showed mainly expansion/contraction of the lateral ventricles without little change of gyri or sulci. At this step the scalp was removed using the automated skull-stripping algorithm brain extraction tool (BET).<sup>20</sup>

Subsequently, scans were segmented into grey matter (GM), white matter (WM) and CSF, based on a segmentation algorithm implemented in SPM5 (<http://www.fil.ion.ucl.ac.uk/spm/software/spm5/>) producing statistical probability anatomical maps (SPAMs). We found that this algorithm outperformed the previous SPM implementations, especially in subjects with enlarged ventricles.

SPAMs values range from 0% to 100% probability of a voxel belonging to a tissue class (GM, WM, and CSF). Registration accuracy was enhanced by aligning and scaling with advanced registration methods spreading registration bias among the whole group – transformation matrix averaging by projection on a manifold.<sup>8,21</sup> Finally, grey matter volumes were smoothed with a Gaussian

kernel of 12 mm (full-width at half maximum-FWHM), a kernel which seems to perform well in studies of simulated atrophy (best kernels being in the range of 10-15mm).<sup>22</sup>

### **Image level Statistics: statistical parametric mapping (SPM)**

Initially an SPM two-sample t-test was applied to search for grey matter differences between the two groups. Statistics were run within a brain mask excluding the cerebellum (mask created with the 'aal' toolbox, see below). Since the baseline clinical measures were unbalanced at baseline we further refined the statistical model by including age, gender, and NYU and SIENAX global grey matter volume in the model (model: "single-subject, conditions and covariates" with the modeled variables introduced as nuisance variables). NYU was preferred over MMSE since in a logistic regression model with NYU and MMSE as predictors and conversion as outcome, it was only NYU which remained significantly independent ( $p_{\text{NYU}}=0.05$ [OR 2.3,1-5.2] versus  $p_{\text{MMSE}}=0.15$ [OR 2.8, 0.7-11]). CDR was not entered in the model since it practically represents a binary outcome. Visual scoring of MTA was also not included in the model since it is highly correlated with SPAM data (both derived from the same source images). Our threshold for statistical significance was set to  $p<0.001$  uncorrected for multiple comparisons, subsequently suprathreshold voxels were further filtered to  $p<0.1$  corrected with FDR (false discovery rate) for multiple comparisons and cluster height  $p<0.1$  corrected for multiple comparisons.

### **Variable level Statistics**

T-tests were performed where appropriate. Monte-Carlo nonparametric statistical simulation was applied to test for differences in visual scores, and NYU score (exact p values). Fisher's exact test was used to compare sex proportions between the two groups.



**Table 1. VBM method protocol.**

VBM	Action	Algorithm
Step 1: preprocessing	Affine register to MNI template	SPM5
	Skull strip images	BET
	Segment grey matter	SPM5
Step 2: Statistics	Manifold additional affine registration	air, define_commonair
	1. Simple t-test between converters and non-converters	SPM5
	2. Model with covariates	SPM5
	Condition: conversion or not	
	Nuisance variables: age, sex, global grey matter, NYU	
	MMSE not included due to significant interaction with NYU	
	3. Reporting of results at $p < 0.1$ corrected and anatomical percentages	Aal

SPM: Statistical Parametric Mapping (software, versions SPM2 and SPM5), air: automated image registration, MNI: Montreal Neurological Institute, BET: brain extraction tool, NYU: delayed New York paragraph recall, MMSE: mini-mental state examination, aal: automatic anatomic labeling toolbox.

## Technical Issues

(<http://www.fil.ion.ucl.ac.uk/spm/software/spm2/>) running under Matlab 6.5 (The Mathworks, MA). The segmentation algorithm was performed with SPM5 (<http://www.fil.ion.ucl.ac.uk/spm/software/spm5/>). Custom image processing steps and batch analysis were coded in IDL 6.1 (Research Systems, CO). Cluster extraction was performed with the SPM plug-in 'marsbar' version 0.38.2.<sup>23</sup> Calculation of cluster locations was performed with the 'aal' toolbox.<sup>24</sup> The 'aal' toolbox parcellates statistical parametric clusters to sub-clusters according to standard-space anatomical boundaries and gives percentage points of each sub-cluster. Conversion of MNI to Talairach coordinates was performed with the mni2tal.m script in Matlab. Special Matlab, IDL and UNIX shell scripts were used to batch process the analysis. All extra scripts and source code is freely available upon request from the author. Conventional statistics were performed with SPSS 13.

## Results

### Baseline Demographics

At the end of the three-year follow-up period 46% of the MCI patients had converted to AD. There were no differences between groups in age or sex (Table 2). MMSE values were relatively high in both groups (above 25), but the patients who progressed to AD differed significantly from the patients who remained stable MCI in terms of lower MMSE and NYU.

**Table 2. Demographics and clinical findings at baseline.**

	MCI non-Converters	MCI Converters
Sample size	13	11
Sex (women/men)	10/3	8/3 (ns)
Age mean (SD, range)	72.4 (8.6, 54-82)	72.7 (4.8, 66-79)
MMSE score (SD, range)	27.5(1.4, 26-30)	25.9(0.9, 24-28)*
NYU score (SD, range)	4.4(3, 0-10)	0.7(1.3, 0-4)*
CDR (n subjects)	2 with CDR 0 11 with CDR 0.5	5 with CDR 0 4 with CDR 0.5 2 with CDR 1

MCI = mild cognitive impairment, MMSE = mini-mental scale examination, NYU = delayed New York paragraph recall, ns= not significant. \* p < 0.01

### MTA and cortical atrophy

The converters exhibited more medial temporal lobe atrophy already at baseline, according to visual scoring of medial temporal lobe atrophy by using a well-validated method.<sup>15,16</sup> The median difference was one step on the MTA rating scale, with the non-converters displaying a median score of 1 and the converters a median score of 2. Global brain grey matter volumes as evaluated by SIENAX demonstrated 5% less total grey matter volume in the converters.

**Table 3. Descriptive MRI results.**

	MCI non-Converters	MCI Converters
Medial Temporal Lobe Atrophy score, Left	1 (1.5)	2 (2)*
Medial Temporal Lobe Atrophy score, Right	1 (1.5)	2 (1)*
Grey Matter volume in cm <sup>3</sup>	695 (51, 624-805)	657 (34, 597-709)*

The first two variables are expressed as median with interquartile range (quartile-3 minus quartile-1). The last two variables are expressed as mean with standard deviation and range.

\* p <0.05

### VBM results

The patients who progressed to AD were found to have more atrophic left medial and lateral temporal lobe structures, left parietal lobe structures and right lateral temporal lobe structures (figure 1). Anatomical parcellation of the clusters allowed evaluation of percentage of clusters of significant differences according to anatomical regions (Table 4). The left medial temporal lobe structures involved were the hippocampus, parahippocampal gyrus, fusiform gyrus and amygdala (highest percentage for the hippocampus and parahippocampal gyrus). The involved left lateral temporal lobe structures included the superior and middle temporal gyrus, and the superior and middle temporal pole (highest percentages for the superior and middle temporal gyrus). The left parietal lobe structures involved were the angular gyrus, inferior parietal lobule and the supramarginal gyrus (highest percentages for the angular gyrus and the inferior parietal lobule). The involved right lateral

temporal lobe structures included the superior, middle and inferior temporal gyrus, and the superior and middle temporal lobe (highest percentages for the middle and superior temporal gyrus). Figure 1 shows the unthresholded VBM maps (with a color-coded significance scale).

After correction for age, gender, global grey matter volume, and delayed NYU the overall statistical significance declined with only left-sided atrophy surviving the statistical threshold, namely parietal atrophy (angular gyrus and inferior parietal lobule) and lateral temporal lobe atrophy (superior and middle temporal gyrus). These results indicate that location of (more) atrophy in those regions carries independent predictive value for conversion to AD.

**Table 4. VBM results of contrast between MCI converters and MCI non-converters.**

MNI Max	pCluster	K	T	pFDR	Cluster %	R/L	Location
-58 0 -15	0.0001	5240 (5.2 cm <sup>3</sup> )	5.1	0.04	46.51	Left	Superior Temporal Gyrus
					40.88	Left	Middle Temporal Gyrus
					6.16	Left	Superior Temporal Pole
					5.23	Left	Middle Temporal Pole
-24 -4 -24	0.002	3220 (3.2 cm <sup>3</sup> )	4.7	0.04	57.30	Left	Hippocampus
					21.46	Left	Parahippocampal Gyrus
					10.09	Left	Fusiform Gyrus
					6.27	Left	Amygdala
-52 -64 38	0.05	1524 (1.5 cm <sup>3</sup> )	4.7	0.04	4.41	Left	Middle Temporal Pole
					67.78	Left	Angular Gyrus
					29.27	Left	Inferior Parietal Lobule
56 12 -17	0.04	1627 (1.6 cm <sup>3</sup> )	4.5	0.04	2.95	Left	Supramarginal Gyrus
					47.80	Right	Middle Temporal Gyrus
					22.54	Right	Superior Temporal Pole
					16.40	Right	Inferior Temporal Gyrus
					6.63	Right	Superior Temporal Gyrus
					5.12	Right	Middle Temporal Pole

Statistics calculated within a brain mask excluding cerebellum. Thresholding was performed at p<0.0001 (uncorrected) and subsequently only the cluster surviving corrected thresholds reported (p cluster corrected (pCluster) = 0.1, p false discovery rate (pFDR) voxel corrected=0.1, cluster extent = 70 = 0.7 cm<sup>3</sup>)

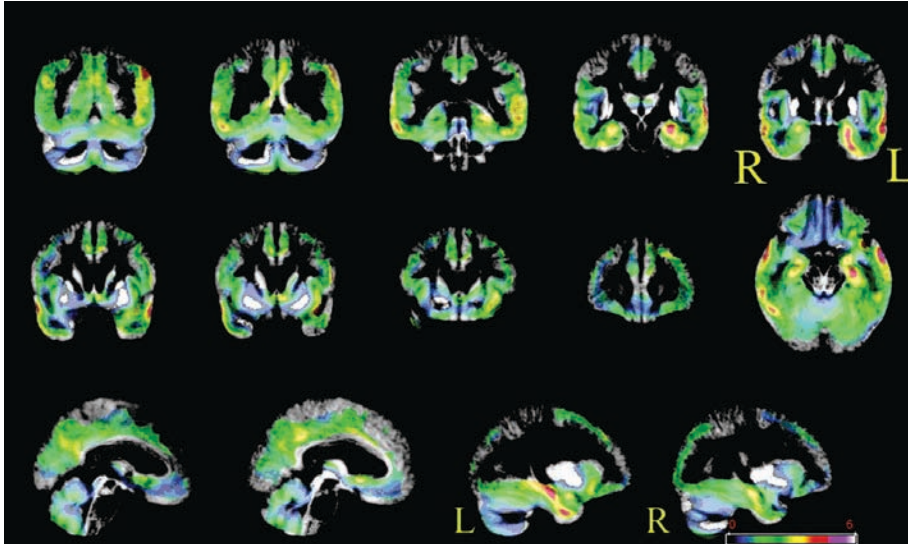


Figure 1. VBM contrast between converters and non-converters using a simple t-test (no covariates). Areas with more atrophy in converters are superimposed on the average grey matter template. No threshold is applied, so that the full extent of the results can be appreciated. Converters have more atrophy of the medial and lateral temporal lobes bilaterally, of frontal lobes and parietal lobes. Thresholded results and corrected for multiple comparisons using random field theory are displayed in tables 4 and 5.

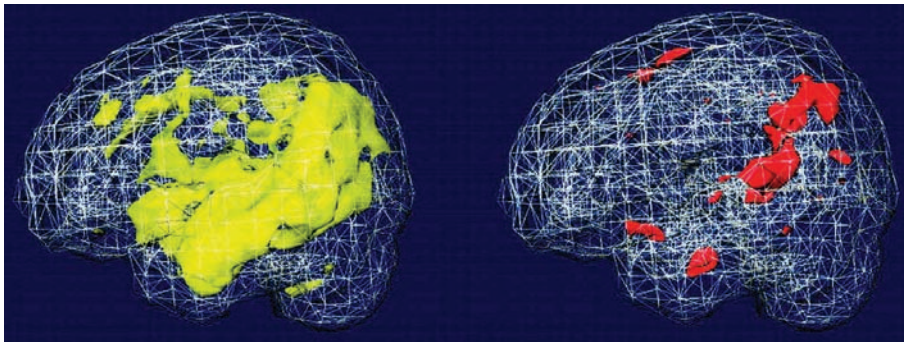


Figure 2. Rendering of the simple t-test and full model (corrected for age, sex, NYU and global grey matter) between MCI converters and non-converters. The big yellow area on the left hemisphere denotes less gray matter (more atrophy) in the converters group, compared to non-converters, as captured by the t-test. After correcting for age, sex, global grey matter atrophy and a neuropsychological measure which is a good predictor of conversion to AD (NYU), atrophy in the left lateral temporal lobe and left parietal regions remains statistically significant, depicted as red. Results were thresholded at  $p=0.001$  uncorrected for multiple comparisons for display purposes.

**Table 5. VBM results of the comparison between MCI converters and MCI non-converters adjusting for gender, age, global grey matter volume and delayed NYU paragraph recall.**

MNI Max	pCluster	K	T	pFDR	Cluster %	R/L	Location
-34 -57 51	0.07	931 (0.9 cm3)	5	0.06	70.03 29.22	Left Left	Angular Gyrus Inferior Parietal Lobule
-54 -42 10	0.06	941 (0.9 cm3)	4.4	0.06	81.08 18.92	Left Left	Superior Temporal Gyrus Middle Temporal Gyrus

Statistics calculated within a brain mask comprising only of temporal and parietal lobes. Thresholding was performed at  $p < 0.0001$  (uncorrected) and subsequently only the cluster surviving corrected thresholds reported (p cluster corrected = 0.1 (pCluster), p false discovery rate (pFDR) voxel-level corrected=0.1, cluster extent = 70 = 0.7 cm3).

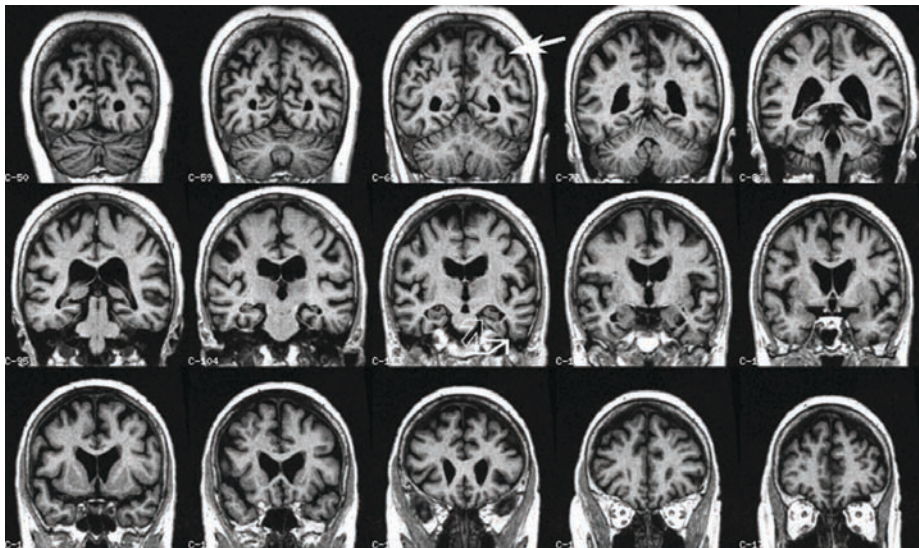


Figure 3. Coronal multiplanar reconstructions of a structural T1-weighted MRI volume. There is slight hippocampal atrophy (open arrow) with concomitant widening of the collateral sulcus (closed kinked arrow), both signs of progressive medial temporal lobe atrophy. We additionally notice slight parietal atrophy (closed arrow), which adds independent predictive value for conversion from mild cognitive impairment to Alzheimer’s disease.

### Discussion

Our goal in this study was to test whether prediction of conversion by utilization of clinical variables can be augmented by incorporating structural imaging data. Almost half (46%) of the MCI amnesic population had deteriorated to fulfill diagnostic criteria for AD, comparable with previous studies on the conversion rate in MCI.<sup>2</sup> We found that medial and lateral temporal lobe atrophy as well as parietal cortex atrophy on MRI characterized converters (figure 1). After correction for clinical variables, left lateral temporal and left parietal cortex atrophy conveyed independent predictive value to distinguish converters from non-converters (figures 2 and 3). Of note, hippocampal atrophy was not significant after correction for the above variables. The importance of lateral parietal cortex atrophy might be significant since it is believed to be mainly involved at a later stage of the disease and not in MCI. Introduction of a visual scoring method for evaluation of medial temporal lobe atrophy might appear coarse, but its use offers robustness to our findings since the visual scale used has been well validated.<sup>15,16</sup>

The finding of medial and lateral temporal lobe atrophy in the patients who progressed to AD is in agreement with previous MRI studies.<sup>4, 16, 25-28</sup> Involvement of both medial and lateral temporal lobes corresponds to neuropathological Braak stages III and IV, the time when there is disruption between the two hemispheres and cognitive deterioration first becomes apparent.<sup>29</sup> There are only few published studies using VBM to study MCI conversion. One study (n=18) with a conversion rate of 39% over 18 months, found more atrophy of medial and lateral temporal lobe structures, and frontal lobe gyri in converters<sup>25</sup>. Another study (n=9) with a conversion rate of 44% at 45.7 months, found more atrophy of medial and lateral temporal lobe structures and the frontal lobe in converters.<sup>26</sup> We did not notice frontal lobe atrophy to the extent described in the other two VBM studies. A possible explanation might be that frontal lobe atrophy did not survive the statistical threshold: it is visible on the unthresholded VBM maps (figure 1).

Moving further away from the temporal lobe, we also noted parietal atrophy. Especially after correcting our data for a measure of disease severity it was only left-sided parietal atrophy and lateral temporal atrophy which distinguished



converters from non-converters. Parietal atrophy is known to characterize AD. Neuropathologically, involvement of the parietal cortex corresponds to Braak stages V and VI of neurofibrillary tangles (NFTs) deposition, at the time usually the diagnosis of AD is made.<sup>29</sup> It seems that functional changes in the parietal cortex might even precede tissue loss.<sup>30</sup> The first data of parietal cortex involvement in MCI developing AD came from studies utilizing PET and SPECT.<sup>6, 31-34</sup> A goal for future research might be to correlate *in vivo* data, pathological data and clinical status of MCI patients to determine the precise contribution of parietal atrophy or hypometabolism to MCI status.

The strength of this study lies in the unbiased way of identifying atrophic brain regions. Additionally, we showed that even after accounting for clinical variables there remained brain atrophy to discriminate patients who would later develop AD. One could argue that the two groups were already clinically different at baseline and that we simply detected AD patients at different stages of the disease. That may very well be true and putting arbitrary cutoffs on a continuum might indeed be controversial. On the other hand, our main goal was not to find isolated regions of brain atrophy in patients with equal cognitive status; clinical scales are well known for their strong predictive ability and it might be naive to think that structural MRI is able to discriminate among the very mild patients. More relevant is the survival of brain atrophy locations after correcting for the predictive ability of clinical scales. As our sample size was relatively small a larger study is needed to confirm the findings and usefulness of lateral temporal and parietal atrophy. Moreover, VBM has caused controversy<sup>35,36</sup>, and additional studies utilizing a different post-processing approach are needed to corroborate our findings. Unfortunately a region of interest approach (considered the gold standard for the hippocampus) might be problematic for the parietal region due to high sulcal variability in that region.<sup>37</sup> VBM smoothes gyri, thereby reducing this variability and enabling comparisons. Another strength of this study is the relatively long follow-up of 3 years and ascertainment of conversion. Nevertheless, one could argue that with even longer follow-up more MCI patients would deteriorate; most likely those will have less severe disease. A more elegant approach would have been to implement survival analysis in VBM and utilize time to conversion and not



a dichotomous criterion. Unfortunately, no such algorithm implementation of survival models in VBM exists to our knowledge and is beyond the capabilities and resources of our research group.

### **Conclusion**

By studying two MCI populations, converters versus non-converters, we found atrophy beyond the medial temporal lobe to be characteristic of MCI patients who will progress to dementia. Atrophy of structures such as the left lateral temporal lobe and left parietal cortex may independently predict conversion.

## Reference list

1. Petersen RC. Mild cognitive impairment as a diagnostic entity. *J Intern Med* 2004;256:183-194
2. Petersen RC, Doody R, Kurz A, et al. Current concepts in mild cognitive impairment. *Arch Neurol* 2001;58:1985-1992
3. Grundman M, Jack CR, Jr., Petersen RC, et al. Hippocampal volume is associated with memory but not nonmemory cognitive performance in patients with mild cognitive impairment. *J Mol Neurosci* 2003;20:241-248
4. Jack CR, Jr., Shiung MM, Weigand SD, et al. Brain atrophy rates predict subsequent clinical conversion in normal elderly and amnesic MCI. *Neurology* 2005;65:1227-1231
5. Baron JC, Chetelat G, Desgranges B, et al. *In vivo* mapping of gray matter loss with voxel-based morphometry in mild Alzheimer's disease. *Neuroimage* 2001;14:298-309
6. Chetelat G, Desgranges B, De La Sayette V, Viader F, Eustache F, Baron JC. Mild cognitive impairment: Can FDG-PET predict who is to rapidly convert to Alzheimer's disease? *Neurology* 2003;60:1374-1377
7. Pennanen C, Testa C, Laakso MP, et al. A voxel based morphometry study on mild cognitive impairment. *J Neurol Neurosurg Psychiatry* 2005;76:11-14
8. Karas GB, Scheltens P, Rombouts SA, et al. Global and local gray matter loss in mild cognitive impairment and Alzheimer's disease. *Neuroimage* 2004;23:708-716
9. van der Flier WM, van den Heuvel DM, Weverling-Rijnsburger AW, et al. Magnetization transfer imaging in normal aging, mild cognitive impairment, and Alzheimer's disease. *Ann Neurol* 2002;52:62-67
10. Devanand DP, Pradhaban G, Liu X, et al. Hippocampal and entorhinal atrophy in mild cognitive impairment: prediction of Alzheimer disease. *Neurology* 2007;68:828-836
11. Apostolova LG, Dutton RA, Dinov ID, et al. Conversion of mild cognitive impairment to Alzheimer disease predicted by hippocampal atrophy maps. *Arch Neurol* 2006;63:693-699
12. Folstein MF, Folstein SE, McHugh PR. "Mini-mental state". A practical method for grading the cognitive state of patients for the clinician. *J Psychiatr Res* 1975;12:189-198
13. McKhann G, Drachman D, Folstein M, Katzman R, Price D, Stadlan EM. Clinical diagnosis of Alzheimer's disease: report of the NINCDS-ADRDA Work Group under the auspices of Department of Health and Human Services Task Force on Alzheimer's Disease. *Neurology* 1984;34:939-944

## Chapter 2

14. Morris JC. Clinical dementia rating: a reliable and valid diagnostic and staging measure for dementia of the Alzheimer type. *Int Psychogeriatr* 1997;9 Suppl 1:173-176; discussion 177-178
15. Scheltens P, Leys D, Barkhof F, et al. Atrophy of medial temporal lobes on MRI in "probable" Alzheimer's disease and normal ageing: diagnostic value and neuropsychological correlates. *J Neurol Neurosurg Psychiatry* 1992;55:967-972
16. Korf ES, Wahlund LO, Visser PJ, Scheltens P. Medial temporal lobe atrophy on MRI predicts dementia in patients with mild cognitive impairment. *Neurology* 2004;63:94-100
17. Smith SM, Zhang Y, Jenkinson M, et al. Accurate, robust, and automated longitudinal and cross-sectional brain change analysis. *Neuroimage* 2002;17:479-489
18. Ashburner J, Friston KJ. Voxel-based morphometry--the methods. *Neuroimage* 2000;11:805-821
19. Karas GB, Burton EJ, Rombouts SA, et al. A comprehensive study of gray matter loss in patients with Alzheimer's disease using optimized voxel-based morphometry. *Neuroimage* 2003;18:895-907
20. Smith SM. Fast robust automated brain extraction. *Hum Brain Mapp* 2002;17:143-155
21. Woods RP. Characterizing volume and surface deformations in an atlas framework: theory, applications, and implementation. *Neuroimage* 2003;18:769-788
22. Davatzikos C, Genc A, Xu D, Resnick SM. Voxel-based morphometry using the RAVENS maps: methods and validation using simulated longitudinal atrophy. *Neuroimage* 2001;14:1361-1369
23. Brett M, Anton JL, Valabregue R, Poline JB. Region of interest analysis using an SPM toolbox. 8th International Conference on Functional Mapping of the Human Brain. Sendai, Japan; 2002
24. Tzourio-Mazoyer N, Landeau B, Papathanassiou D, et al. Automated anatomical labeling of activations in SPM using a macroscopic anatomical parcellation of the MNI MRI single-subject brain. *Neuroimage* 2002;15:273-289
25. Chetelat G, Landeau B, Eustache F, et al. Using voxel-based morphometry to map the structural changes associated with rapid conversion in MCI: a longitudinal MRI study. *Neuroimage* 2005;27:934-946
26. Bell-McGinty S, Lopez OL, Meltzer CC, et al. Differential cortical atrophy in subgroups of mild cognitive impairment. *Arch Neurol* 2005;62:1393-1397

27. deToledo-Morrell L, Stoub TR, Bulgakova M, et al. MRI-derived entorhinal volume is a good predictor of conversion from MCI to AD. *Neurobiol Aging* 2004;25:1197-1203
28. Killiany RJ, Hyman BT, Gomez-Isla T, et al. MRI measures of entorhinal cortex vs hippocampus in preclinical AD. *Neurology* 2002;58:1188-1196
29. Braak E, Griffing K, Arai K, Bohl J, Bratzke H, Braak H. Neuropathology of Alzheimer's disease: what is new since A. *Alzheimer? Eur Arch Psychiatry Clin Neurosci* 1999;249 Suppl 3:14-22
30. Chetelat G, Desgranges B, De La Sayette V, et al. Dissociating atrophy and hypometabolism impact on episodic memory in mild cognitive impairment. *Brain* 2003;126:1955-1967
31. Borroni B, Anchisi D, Paghera B, et al. Combined <sup>99m</sup>Tc-ECD SPECT and neuropsychological studies in MCI for the assessment of conversion to AD. *Neurobiol Aging* 2006;27:24-31
32. Drzezga A, Grimmer T, Riemenschneider M, et al. Prediction of individual clinical outcome in MCI by means of genetic assessment and (18)F-FDG PET. *J Nucl Med* 2005;46:1625-1632
33. Drzezga A, Lautenschlager N, Siebner H, et al. Cerebral metabolic changes accompanying conversion of mild cognitive impairment into Alzheimer's disease: a PET follow-up study. *Eur J Nucl Med Mol Imaging* 2003;30:1104-1113
34. Anchisi D, Borroni B, Franceschi M, et al. Heterogeneity of brain glucose metabolism in mild cognitive impairment and clinical progression to Alzheimer disease. *Arch Neurol* 2005;62:1728-1733
35. Ashburner J, Friston KJ. Why voxel-based morphometry should be used. *Neuroimage* 2001;14:1238-1243
36. Bookstein FL. "Voxel-based morphometry" should not be used with imperfectly registered images. *Neuroimage* 2001;14:1454-1462
37. Thompson PM, Mega MS, Woods RP, et al. Cortical change in Alzheimer's disease detected with a disease-specific population-based brain atlas. *Cereb Cortex* 2001;11:1-16

